UBE3D Is Involved in Blue Light-Induced Retinal Damage by Regulating Double-Strand Break Repair

Ningda Xu,[1] Yue Liu,[2] Shanshan Nai,[2] Yong Tao,[3] Yuehe Ding,[4] Lemei Jia,[4] Qizhi Geng,[2] Jie Li,[2] Yujing Bai,[1] Gong-Hong Wei,[5,6] Meng-Qiu Dong,[4] Linyi Luo,[7] Mingwei Zhao,[1] Xingzhi Xu,[2,8] Xiao-Xin Li,[1,9] Jing Li,[2] and Lvzhen Huang[1]

[1]Department of Ophthalmology, Eye Diseases and Optometry Institute, Beijing Key Laboratory of Diagnosis and Therapy of Retinal and Choroid Diseases, College of Optometry, Peking University Health Science Center, Peking University People's Hospital Beijing, China
[2]Beijing Key Laboratory of DNA Damage Response and College of Life Science, Capital Normal University, Beijing, China
[3]Department of Ophthalmology, Beijing Chaoyang Hospital, Capital Medical University, Chaoyang District, Beijing, China
[4]National Institute of Biological Sciences, Beijing, China
[5]Biocenter Oulu, Faculty of Biochemistry and Molecular Medicine, University of Oulu, Oulu, Finland
[6]Department of Biochemistry and Molecular Biology, School of Basic Medical Sciences, Fudan University Shanghai Cancer Center, Shanghai Medical College of Fudan University, Shanghai, China
[7]Department of Ophthalmology and Visual Sciences, Affiliated Dongguan Hospital, Southern Medical University, Guangdong, China
[8]Guangdong Key Laboratory of Genome Stability & Disease Prevention, Shenzhen University School of Medicine, Shenzhen, Guangdong, China
[9]Department of Ophthalmology, Xiamen Eye Center of Xiamen University, Xiamen, China

Correspondence: Lvzhen Huang, Department of Ophthalmology, Eye Diseases and Optometry Institute, Beijing Key Laboratory of Diagnosis and Therapy of Retinal and Choroid Diseases, College of Optometry, Peking University Health Science Center, Peking University People's Hospital, Beijing 100044, China; huanglvzhen@126.com.
Jing Li, Beijing Key Laboratory of DNA Damage Response, College of Life Sciences, Capital Normal University, Beijing 100048, China; jing_li@mail.cnu.edu.cn.
Xiao-Xin Li, Department of Ophthalmology, Eye Diseases and Optometry Institute, Beijing Key Laboratory of Diagnosis and Therapy of Retinal and Choroid Diseases, College of Optometry, Peking University Health Science Center, Peking University People's Hospital, Beijing 100044, China; drlixiaoxin@163.com.

NX, YL, SN, and YT contributed equally to this work.

Received: April 12, 2022
Accepted: August 18, 2022
Published: September 12, 2022

Citation: Xu N, Liu Y, Nai S, et al. UBE3D is involved in blue light-induced retinal damage by regulating double-strand break repair. *Invest Ophthalmol Vis Sci.* 2022;63(10):7. https://doi.org/10.1167/iovs.63.10.7

Purpose. Age-related macular degeneration (AMD) is currently the leading cause of blindness worldwide. Previously, we identified ubiquitin-protein ligase E3D (UBE3D) as an AMD-associated protein for East Asian populations, and here we further demonstrate that UBE3D could be associated with DNA damage response.

Methods. The established I-SceI-inducible GFP reporter system was used to explore the effect of UBE3D on homologous recombination. Immunoprecipitation-mass spectrometry (MS) was used to explore potential UBE3D−interacting proteins and validated with coimmunoprecipitation assays and the pulldown assays. Micrococcal nuclease (MNase) assays were used to investigate the function of UBE3D on heterochromatin de-condensation upon DNA damage. An aged mouse model of blue light-induced eye damage was constructed, and electroretinography (ERG) and optical coherence tomography (OCT) were performed to compare the differences between wild-type and UBE3D$^{+/-}$ mice.

Results. First, we show that GFP-UBE3D is recruited to damage sites by PCNA, through a PCNA-interacting protein (PIP) box. Furthermore, UBE3D interacts with KAP1 via R377R378 and oxidation of the AMD-associated V379M mutation abolishes KAP1-UBE3D binding. By MNase assays, UBE3D depletion reduces the chromatin relaxation levels upon DNA damage. In addition, UBE3D depletion renders less KAP1 recruitment. Compared with wild type, blue light induces less damage in UBE3D$^{+/-}$ mice as measured by ERG and OCT, consistent with our biochemical results.

Conclusions. Hence, we propose that one potential mechanism that UBE3D-V379M contributes to AMD pathogenesis might be via defective DNA damage repair linked with oxidative stress and our results offered a potential direction for the treatment of AMD.

Keywords: age-related macular degeneration (AMD), double-strand break repair (DSBR), KAP1, heterochromatin, methionine oxidation, ubiquitin-protein ligase E3D (UBE3D)

One leading cause contributing to irreversible central blindness among the elderly is age-related macular degeneration (AMD),[1] which in the United States alone affects approximately 10 million people. Its manifestations include lipid-rich extracellular drusen, inflammation, and macula neurodegeneration.[2] The causing factors are multifaceted: defects in lipid transfer and recycling, dysfunctional mitochondria and stress response; lesions in phagocytosis, protein degradation, and molecular transport; aberrant extracellular matrix remodeling; complement activation or chronic inflammation[2]; as well as aging-induced parainflammatory response.[3] Proteins involved in these pathways have been implicated in AMD pathogenesis.

Intriguingly, the AMD-susceptible genes are ethnic-specific. Previously, we utilized whole-exome sequencing and identified that among the East Asian patients with AMD, one genetically predisposed factor is a ubiquitin protein ligase E3D (UBE3D)-V379M single nucleotide variant (SNV).[4] But its underlying mechanism remains enigmatic. UBE3D (also called Ube2CBP or H10BP) was first discovered in a yeast 2-hybrid analysis for proteins that interact with UbcH10, an E2 for the anaphase promoting complex/cyclosome (APC/C).[5] UBE3D is an E3 ligase, containing a homologous to E6-AP carboxyl terminus (HECT) domain at its C terminus, which binds and ubiquitinates cyclin B in vitro.[5] But other substrates as well as its biological functions remain unexplored.

The DNA damage response network is complex and comprises a network of various repair pathways.[6] Double-strand break (DSB) is the most dangerous type of damage, and it must be repaired either through homologous recombination or non-homologous end joining. During the cell cycle, homologous recombination functions in the S and G2 phases and plays a major role in the repair of replication-associated DSBs. On the contrary, non-homologous end joining occurs predominantly in G0/G1 and G2.[6]

DSBs occurring in the context of heterochromatin have to be dealt with in a special manner.[7] Non-homologous end joining is less favorable in the heterochromatin region due to chromatin compaction, hence de-condensation is instrumental to recruit homologous recombination factors and subsequent DSB repair.[8] Mechanistically, heterochromatin DSB repair is delayed than euchromatin and modulated by an ataxia-telangiectasia mutated (ATM)- and KAP1- dependent pathway.[9] Specifically, ATM phosphorylates KAP1 at S824 at the damage sites upon DSBs, and then phosphorylated KAP1 attenuates association with nuclease-resistant chromatin[10] and spreads globally throughout the genome, resulting in chromatin relaxation.[9] Thus, KAP1 knockdown could alleviate the requirement for ATM during DSB repair.[10]

Here, we carried out in-depth studies of UBE3D, and identified some of its binding partners to be critical components of the DNA damage repair network. UBE3D is recruited to DSB sites via a PIP (PCNA-interacting protein) box, and R377R378 are vital for its interaction with KAP1. The AMD-associated SNV, V379M, could easily be oxidized to methionine sulfoxide (MetSO) during oxidative stress, thus mediating dissociation of UBE3D from KAP1. Micrococcal nuclease (MNase) assays further demonstrate chromatin relaxation defects in UBE3D-depleted cells. Consistent with our molecular studies, UBE3D +/- mice displayed less damage compared with WT as measured by electroretinography (ERG), optical coherence tomography (OCT), and ZO-1 staining in a blue light eye damage AMD model in aged mice. Thus, we propose that heterochromatin DSB repair defects could be conducive to late-onset eye diseases.

Materials and Methods

Ethics Statement

The protocol was approved by the Animal Use and Ethical Committee from Peking University People's Hospital and experiments were according to Association for Research in Vision and Ophthalmology Statement of Animal Use. Ethic approval number: 2019PHE059, date: November 28, 2019.

Cell Culture, Antibodies, and Plasmids

HeLa, HEK293, and ARPE-19 cells were purchased from ATCC. Antibodies used: rabbit anti-UBE3D (Abnova, #PAB21883), rabbit anti-PCNA (CST, #D3H8P), mouse anti-FLAG (Sigma-Aldrich, # F1804), and rabbit anti-KAP1 (Abcam, #ab10483). *UBE3D* gene sequences were amplified by PCR and cloned into pcDNA3.0-3HA or -3Flag, generating pcDNA-3HA-UBE3D and pcDNA-3Flag-UBE3D. The UBE3D-RRAA, -PIPΔ, and V379M mutants were generated using specific primers (sequences available upon request) following the manufacturer's instructions (QuickChange II, Stratagene). The control siRNA oligonucleotides duplex was CONTROLsi: CGUACGCGGAAUACUUCGAdTdT. *UBE3D* siRNA oligonucleotides duplexes were: *UBE3D*-si1: GCA GCA AAG ACC UGA ACU A (Guangzhou RiboBio Co., China). HA-*UBE3D*-res plasmids were constructed targeting *UBE3D* siRNA by site-directed mutagenesis with primer sequences: GAATTTAAGAACCAGTTTGTGGGTCGAAAG ATTTAAACT TCCCCAGTGG.

Transfections and Treatments

HeLa and ARPE-19 cells were transfected twice with a 24-hour interval using Oligofectamine (Invitrogen) according to the manufacturer's instructions. Transfectants were used for further experiments 24 hours after the second transfection. For plasmid transfection, cells were seeded at 50% to 60% confluence/10 cm^2 petri dish and transfected with 7.5 µg of plasmid DNA using FuGene 6 according to the manufacturer's instructions for immunoprecipitation (immunoprecipitation) experiments. Chemicals for this study were: Adriamycin (ADR) was used at 2 µg/mL for 1 hour; Neocarzinostatin (NCS) was used at 200 ng/mL for 1 hour; and Bleomycin (Bleo) was utilized at 10 ug/mL for 1 hour.

Immunoprecipitation and Immunoblotting

Immunoprecipitation and immunoblotting experiments were performed as described before.[11] Briefly, the cells were first transfected with the plasmids or treated with different drugs. Then the cells were collected and washed with PBS, followed by cell lysis in the RIPA buffers.[11] The resultant supernatant was collected and the antibodies were added as needed. After incubation overnight at 4°C, Protein A or G Sepharose was added into the solution and incubated further for 1 hour at 4°C. The immunoprecipitates were then subject to extensive wash, then the pellets after centrifugation were collected and boiled in Sample Buffers. The following primary antibodies were used for immunoblotting: anti-MDC1, anti-GFP, anti-UBE3D, anti-PCNA, anti-KAP1,

Investigative Ophthalmology & Visual Science

anti-HA, and anti-FLAG M2 (Sigma). Peroxidase-conjugated secondary antibodies were from Jackson Immuno Research. Blotted proteins were visualized using the ECL detection system (Amersham). Signals were detected by a LAS-4000, and analyzed using Multi Gauge (Fujifilm). Micrococcal nuclease assays were carried out as previously described.[9] All IP experiments were repeated for at least three times.

Immunofluorescence Imaging

Indirect immunofluorescence imaging was carried out as before.[11] Immunofluorescence staining was performed to detect Flag-UBE3D and KAP1 in ARPE-19 cells. Primary antibodies included antibodies against Flag and KAP1. Nuclei were stained with 4′,6-diamidino-2-phenyl-indole (DAPI, abs47047616). Zeiss LSM 710 confocal microscope (Carl Zeiss Meditec, Inc., Dublin, CA, USA) was used to visualize the slides.

Laser Micro-Irradiation

DNA damage induction by laser was performed as previously described.[12] Briefly, a micropoint system (Andor) was used to generate a 365-nm pulsed nitrogen UV laser (16 Hz pulse, 41% laser output). U2OS cells transfected with GFP-UBE3D-WT or mutants were grown on a thin-glass-bottom dish, and locally irradiated. The micropoint system is coupled to a Nikon A1 confocal imaging system to capture time-lapse images.

Generation of UBE3D$^{+/-}$ Mice

Wild-type C57BL/6 mice (males, 12 months old) were used in the in vivo studies. The CRISPR-mediated heterozygous *UBE3D*-knockout mice (*UBE3D*$^{+/-}$) has been described before[4] and produced by View Solid Biotechnology in Beijing, China. The study was approved by the Ethics Committee of Peking University People's Hospital.

Construction of a Mouse Model With Blue Light Damage

The mice were placed in the dark with food and water for 12 hours, and then exposed to blue light (peak wavelength: 450 µm, 10,000 lux) at 10,000 lux for 12 hours. The pupils were dilated 30 minutes before exposure. After light damage, the mice were restored to a dark environment until the next morning, and then they were restored to a normal 12 hour and 12 hour light-dark cycle.

Electroretinography

The ERG recording system (RETIport, Roland Consult, Germany) was used to record the full-field flash ERG using the standards of the International Visual Clinical Electrophysiology Association. ERG was carried out as previously described.[4] Briefly, all procedures were performed in a dark room under a red light (>650 nm). Under dark-adapted conditions, both eyes obtained flash ERG records at the same time, and the white light stimulation intensity of dark-view ERG was initially set to 0.001 cd s m-2. Then, the intensity was increased to 0.003, 0.3, and 3 cd s m-2. The mice were then acclimatized to light for 15 minutes in the background of bright vision (25 cd s m-2). The stimulation intensity of visual ERG was initially 1 cd s m-2, and then increased to 3 and 10 cd s m-2. At the brightness level above, each record is averaged three times.

Optical Coherence Tomography

UBE3D$^{+/-}$ mice were subject to OCT (Optoprobe 4D-isOCT, test mouse special lens) under anesthesia before the blue light exposure and 5 days after the end of the exposure, as described before.[13] SPSS software version 20.0 (US SPSS, Inc.) was used for data analysis. All data are expressed as mean ± SD. The difference between the experimental group and the control group was tested using Student's *t* test. Any $P < 0.05$ was considered statistically significant.

Zonula Occludens-1 Staining of Retinal Pigment Epithelium

To visualize the integrity of the RPE structure, zonula occludens-1 (ZO-1), staining was performed as previously described.[14] Briefly, mouse RPE/choroid flat mounts were fixed with 4% PFA or 100% methanol, stained with rabbit antibodies against ZO-1 (1:100; Invitrogen, Carlsbad, CA, USA), and visualized with Alexa 594 (Invitrogen). All images were obtained using the Zeiss LSM 710 confocal microscope (Carl Zeiss Meditec, Inc., Dublin, CA, USA).

Results

UBE3D is Required for Homologous Recombination

As the function of UBE3D is unknown, we first utilized siRNA targeting *UBE3D* to deplete it from cells (Fig. 1A). Then, we tried to examine the possibility that UBE3D might be involved in DNA damage repair and utilized the established I-SceI-inducible GFP reporter system[15,16] (Fig. 1B). By transfection with the I-SceI construct, homologous recombination will generate a functional GFP that could be detected by flow cytometry.[15,16] This assay demonstrated that homologous recombination was significantly reduced in UBE3D-knockdown cells (Fig. 1C), suggesting that UBE3D modulates homologous recombination. We then explored whether UBE3D mediates cell viability upon genotoxic stress by clonogenic assays. The survival rate of UBE3D-knockdown cells under Etoposide (ETO) treatment was significantly downregulated (Figs. 1D, 1E). In sum, these data suggest that UBE3D is vital for genome integrity via homologous recombination.

UBE3D Interacts With PCNA Through the PIP Box

To explore potential UBE3D interaction proteins, we used immunoprecipitation-mass spectrometry (MS). We first constructed full-length UBE3D constructs. Flag-UBE3D plasmids were transfected into cells, and the anti-Flag immunoprecipitates were subject to SDS-PAGE and silver staining (Fig. 2A). Among the potential UBE3D-interacting proteins are PCNA and KAP1 (Fig. 2B), which are instrumental for DNA damage repair. As PCNA is the DNA clamp protein,[17] we first tested the interaction between UBE3D and PCNA and found that the interaction between both endogenous

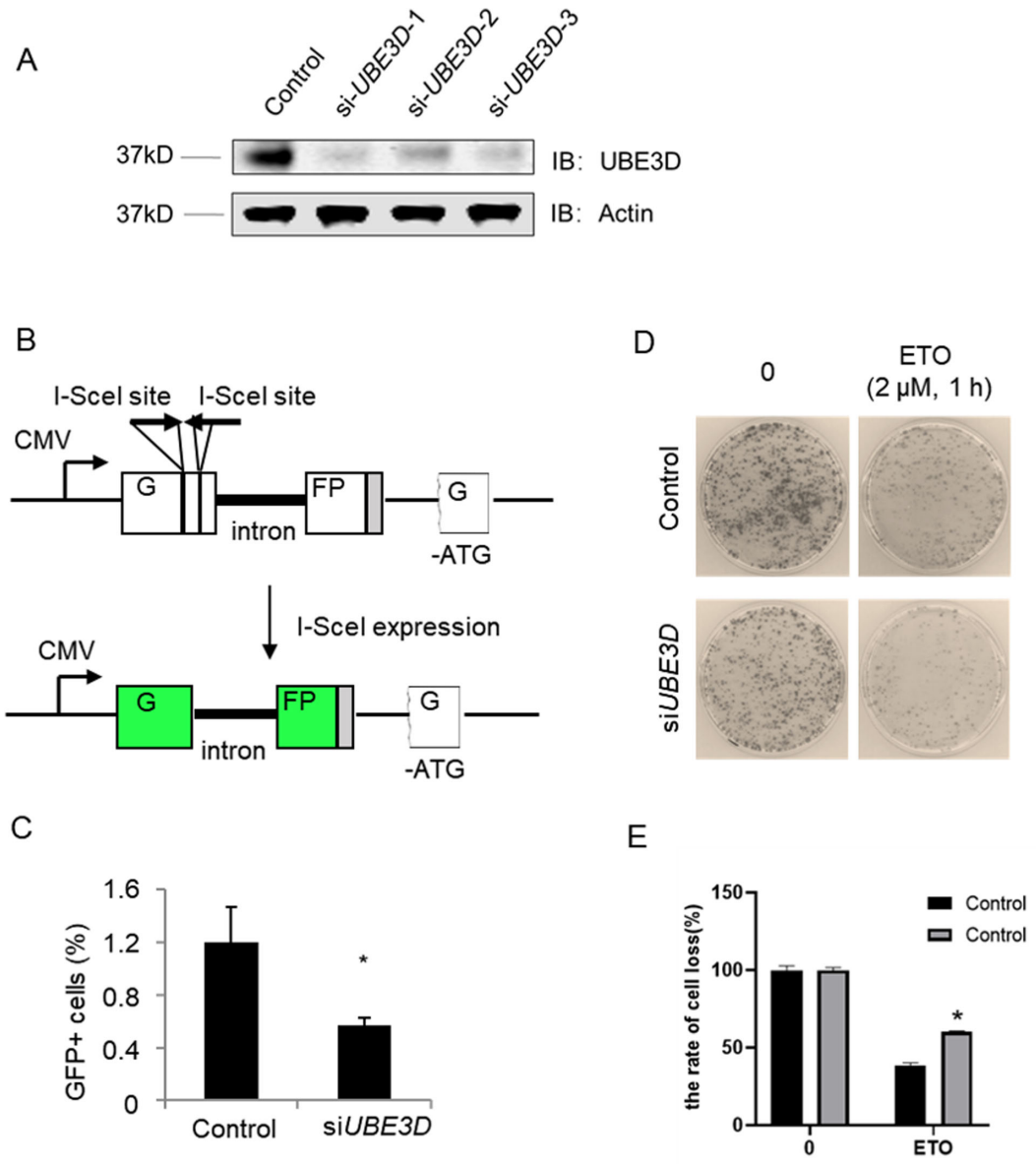

Figure 1. UBE3D protects cells from genotoxic lesions. (**A**) Cells were transfected with siRNA targeting *UBE3D* or control siRNA. The lysates were collected and then immunoblotted with the antibodies indicated. Rabbit anti-UBE3D antibodies: Pab21883, Abnova. (**B**) The GFP-based reporter assay for homologous recombination is deployed as previously described.[15,16,18] Briefly, the homologous recombination cassette comprises of the first exon of GFP harboring two inverted I-SceI restriction sites, followed by a promoter-less first exon that also lacks ATG. Upon I-SceI expression, the construct will produce a functional GFP due to gene conversion events, which are predominant homologous recombination pathways in mammalian cells. (**C**) To monitor the potential role of UBE3D in homologous recombination, the cells described in **B** were depleted of UBE3D by siRNA. Two days later, the cells were analyzed for GFP expression by the FACS assay. The diagram depicts mean ± SD. The asterisk indicates significant difference. (**D**) UBE3D-knockdown cells were exposed to Etoposide (2 μM) for 1 hour. (**E**) Quantitation of **D**.

and ectopic expressed UBE3D and PCNA increased upon DNA damage reagent treatment (Figs. 2C, 2D).

As most PCNA-binding proteins contain a conserved PIP box that is signified by aromatic residues (most often Y or F),[19] we scanned the protein sequence of UBE3D and found F167F168. We then mutated these two amino acids to Ala and generated F167AF168A (PIPΔ) mutants (Fig. 2H). PIPΔ abolished interaction with PCNA in coimmunoprecipitation assays (see Fig. 2D), as well as in the pulldown assays (Fig. 2E), suggesting that F167F168 is indispensable for UBE3D to interact with PCNA.

Then, we sought to address whether UBE3D is recruited to DNA damage sites. By laser-induced DNA lesion approaches, GFP-UBE3D is identified at the damage sites, most predominantly starting from 100 seconds (Fig. 2F), which is relatively slow compared to other damage proteins. PCNA, for instance, was recruited to the damage sites starting from 30 seconds, together with ACF1.[20] The PIPΔ mutant, in sharp contrast, was not identified at the laser cleavage site (see Figs. 2F, 2G), suggesting that the interaction between UBE3D and PCNA is essential for UBE3D recruitment.

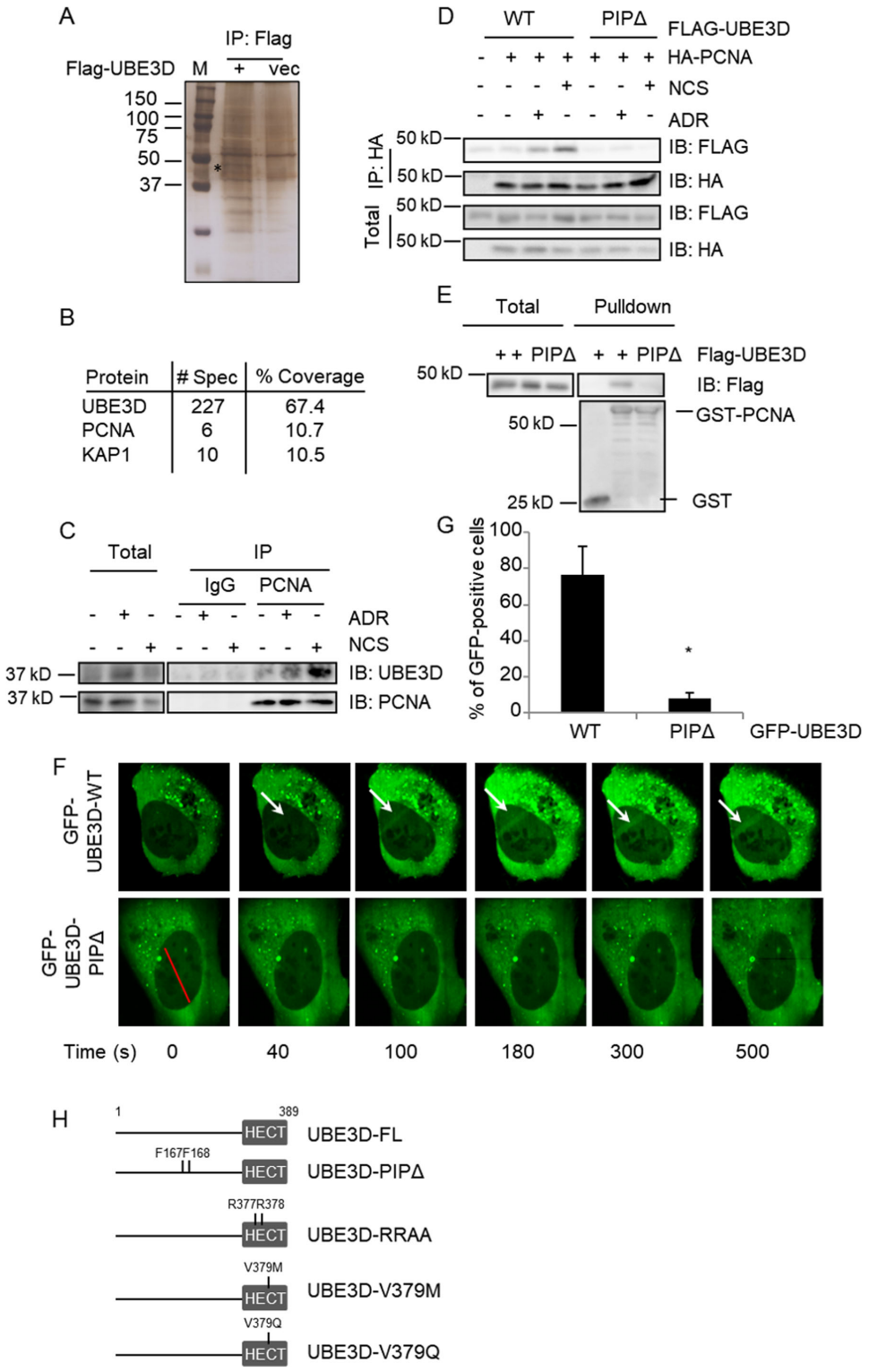

Figure 2. The PIP box of UBE3D is critical for its interaction with PCNA. (**A**) HeLa cells were transfected with Flag-UBE3D. Cell lysates were immunoprecipitated with anti-Flag agarose, then subject to silver staining. *Asterisk* indicates the Flag-UBE3D band. M stands for Marker. (**B**) The immunoprecipitates in **A** were subject to mass spectrometry (MS) analysis to identify UBE3D-interacting proteins. The table showed proteins identified in the MS analysis. The numbers indicate peptides and peptide coverage percentage, respectively. (**C**) HeLa cells were treated with ADR, Neocarzinostatin (NCS), or left untreated. The lysates were immunoprecipitated with anti-PCNA antibodies and immunoblotted with the antibodies indicated. Rabbit anti-PCNA antibodies: D3H8P and CST. (**D**) HeLa cells were transfected with Flag-UBE3D and HA-PCNA, and then treated with ADR, NCS, or left untreated. Then the lysates were subject to immunoprecipitation and immunoblotting as indicated. (**E**) Pull-down experiments using GST-PCNA to pull down transfected Flag-UBE3D-WT or –PIPΔ (PIPΔ refers to F167AF168A that disrupts the interaction between UBE3D and PCNA). (**F**) Cells transfected with GFP-UBE3D-WT or –PIPΔ mutants were laser micro-irradiated. Representative images are shown. The *red line* at the bottom panel indicates where the laser was applied. (**G**) Quantitation of the results in **F**. At least 20 cells were irradiated per experiment. The asterisk indicates significant differences. (**H**) Schematic representation of UBE3D plasmid constructs used in this study.

UBE3D Interacts With KAP1

What strikes us as odd is that human eyes with UBE3D-V379M are susceptible to AMD, but mouse eyes with UBE3D-M379 are WT,[4] suggesting that there are some fundamental distinctions between the two species (Fig. 2H shows the position of UBE3D-V379M in the HECT domain). An in-depth literature search unveiled that rod photoreceptors of mice, which are nocturnal animals, contain an inverted chromatin structure compared to other diurnal animals.[21–23] Usually, heterochromatin is enriched around the nuclear envelop and the nucleoli, with the euchromatin distributed in between.[24] Rod receptors in the retina are the light-sensing cells. The rod receptors of diurnal animals often contain nuclei of the conventionally organized structure, because it is light scattering.[21] In nocturnal animals, which need a strong light-focusing ability, their rod receptors often contain an inverted heterochromatin organization. They harbor a single large chromocenter (consisting of heterochromatins) in the middle, with the euchromatin around the nuclear envelope.[21] This clue hinted to us that UBE3D-V379 or -M379 might be linked to chromatin configuration.

In the MS data, we also identified KAP1 (see Fig. 2B), which is a heterochromatin building block and facilitates heterochromatin DSB repair.[9,25] Moreover, the recruitment of UBE3D is slow, which is consistent with the later repair of heterochromatin DNA damages. Therefore, we sought to examine whether UBE3D associates with KAP1.

We performed immunofluorescence detection on ARPE-19 cells to observe the intracellular localization of UBE3D and KAP1. It was found that the two proteins were highly overlapped in the intracellular spatial position, indicating a strong relationship between the two (Fig. 3E). Endogenous co-immunoprecipitation assays were carried out with

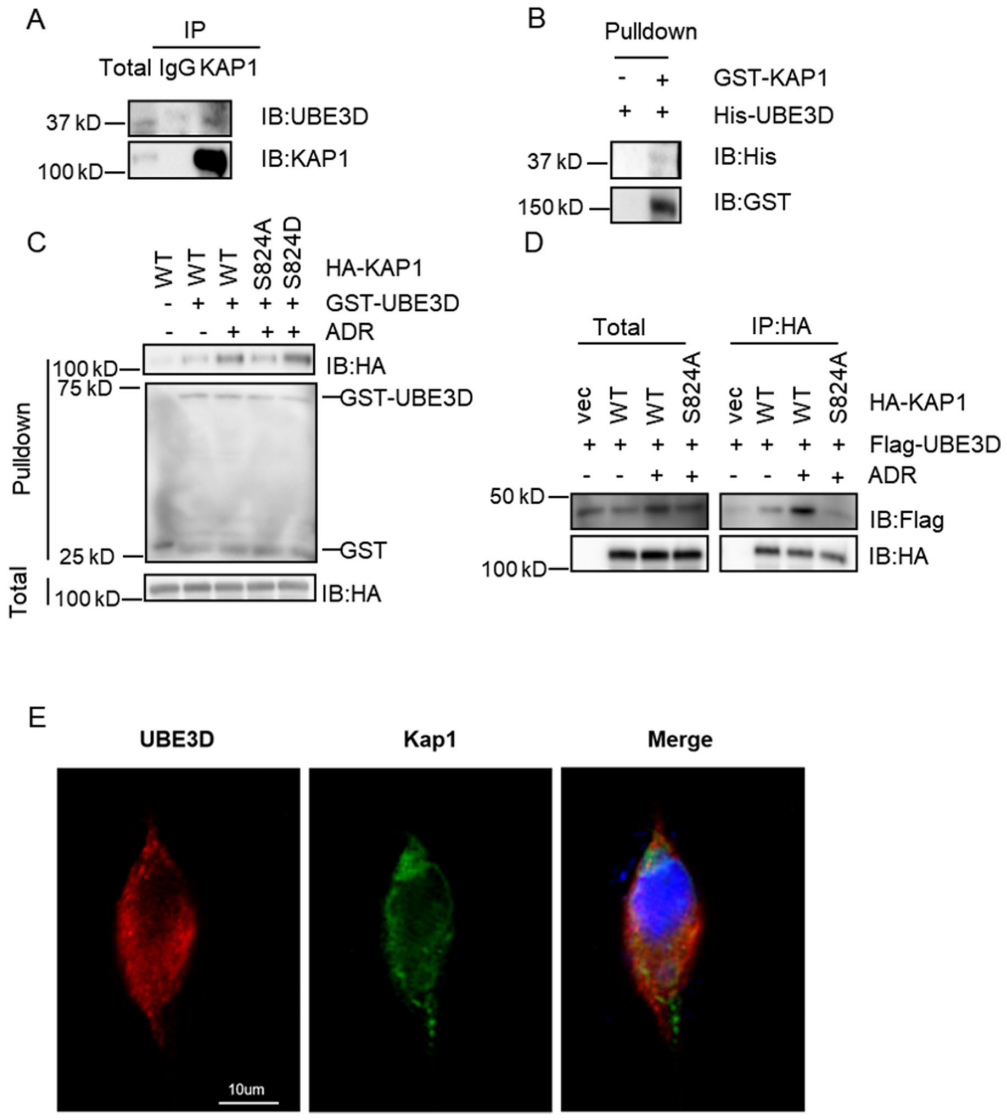

Figure 3. Phosphorylation of KAP1 at S824 is critical for KAP1-UBE3D interaction. (**A**) HeLa cell extracts were immunoprecipitated with anti-KAP1 antibodies and immunoblotted with the antibodies indicated. Rabbit anti-KAP1 antibodies: Ab10483, Abcam. (**B**) His-UBE3D and GST-KAP1 were purified from bacteria and subject to GST pulldown assays. (**C**) HeLa cells were transfected with HA-KAP1-WT, -S824A, or -S824D plasmids and cell lysates were incubated with GST-UBE3D proteins purified from bacteria. (**D**) HeLa cells were transfected with HA-KAP1-WT or -S824A plasmids, together with Flag-UBE3D, then treated with ADR at 2 µg/mL for 1 hour or not treated. The cell extracts were subject to immunoprecipitation and immunoblotting with antibodies indicated. (**E**) ARPE-19 cells were transfected with Flag-UBE3D, and then and the localization of UBE3D and KAP1 in the cells was observed by confocal microscope. Scale bar = 10 µm. UBE3D presented with a red signal and KAP1 presented with a *green* signal.

Investigative Ophthalmology & Visual Science

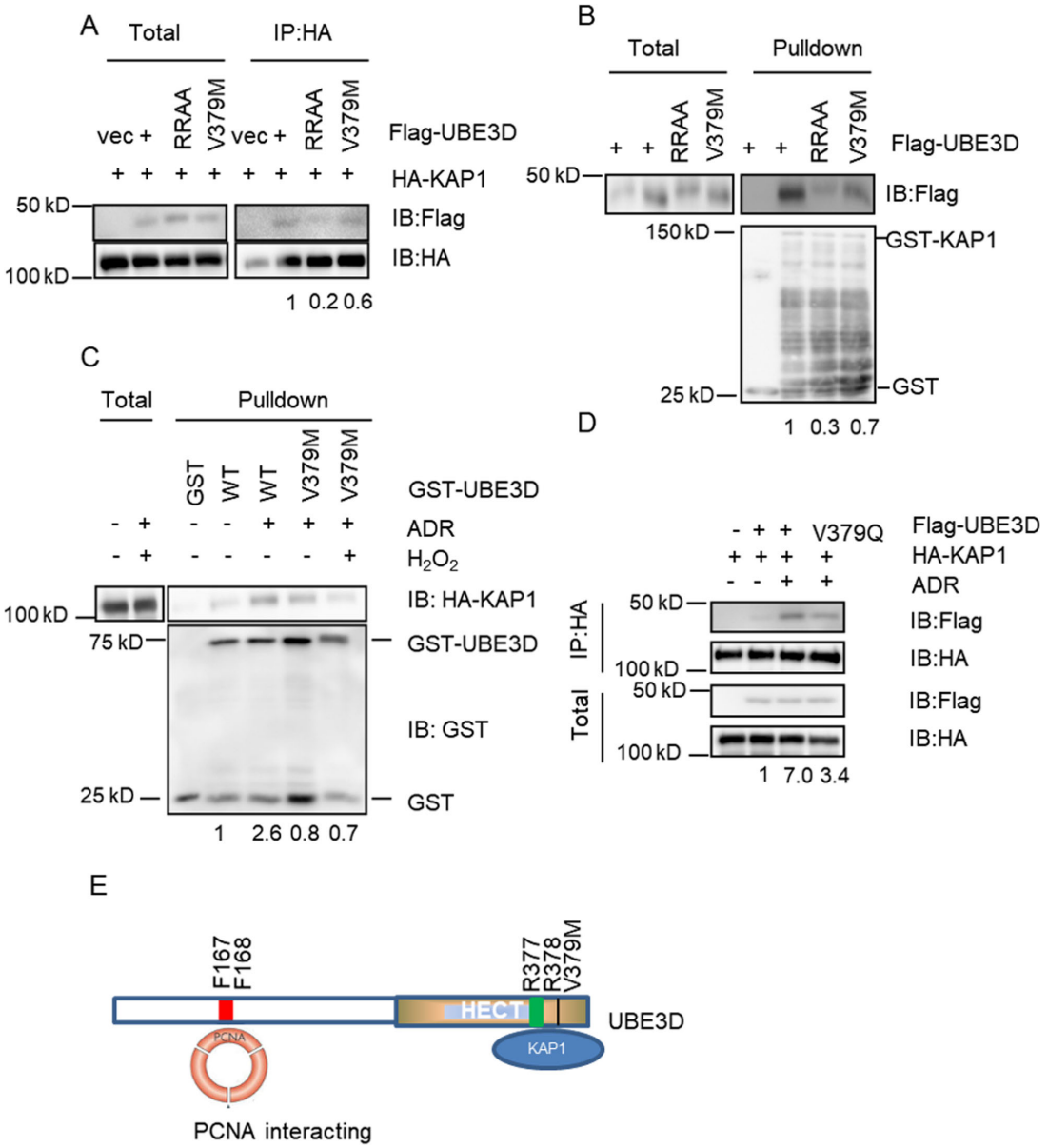

Figure 4. The association between KAP1 and UBE3D hinges upon R377R378. (**A**) HeLa cells were transfected with HA-KAP1 together with Flag-UBE3D-WT, -V379M, -RRAA, or vector controls. The lysates were collected, followed by immunoprecipitation with anti-HA antibodies and immunoblotting with the antibodies indicated. (**B**) GST-KAP1 was purified from *E. coli,* and then incubated with cell lysates containing Flag-UBE3D-WT, RRAA, or V379M plasmids. (**C**) Cells were transfected with HA-KAP1, treated with ADR, and then incubated with GST-UBE3D-WT, and V379M proteins pretreated or not treated with H_2O_2. (**D**) Cells were transfected with HA-KAP1, together with Flag-UBE3D-WT or –V379Q plasmids, treated with ADR or not. Then, the lysates were collected to perform immunoprecipitation and immunoblotting assays. The numbers at the bottom indicate quantitation of the corresponding bands. (**E**) A model depicting UBE3D interaction domains. UBE3D interacts with PCNA with the PIP box (167FF168), which are essential for its recruitment to DSB sites. The 377RR378 motif in the HECT domain is essential for UBE3D to interact with KAP1 and relax heterochromatin during DSB repair, and it also contributes to various cancer types. A V379M mutation abutting the RR motif could be easily oxidized to MetSO, especially during ageing, which abrogates UBE3D-KAP1 interaction, rendering susceptibility to AMD.

anti-KAP1 antibodies, and UBE3D was in the immunoprecipitants (Fig. 3A). GST-KAP1 purified from *E. coli* could pulldown His-UBE3D (Fig. 3B). As KAP1 is phosphorylated by ATM during heterochromatin DSB repair,[9] we wondered whether this phosphorylation event modulates the KAP1-UBE3D interaction. HA-KAP1-S824A and S824D mutants were constructed accordingly and transfected into cells. The cells were then treated with ADR and lysates were collected and incubated with recombinant GST-UBE3D proteins. The GST-UBE3D could pull down HA-KAP1 proteins, and the interaction increased upon ADR treatment (Fig. 3C). KAP1-S824A attenuated interaction with UBE3D, but the S824D mutant did not (see Fig. 3C). We also measured the effect of S824A by co-immunoprecipitation assays, and S824A hindered the association with UBE3D (Fig. 3D). Taken together, UBE3D partners with KAP1, which is facilitated by ATM-dependent phosphorylation at S824.

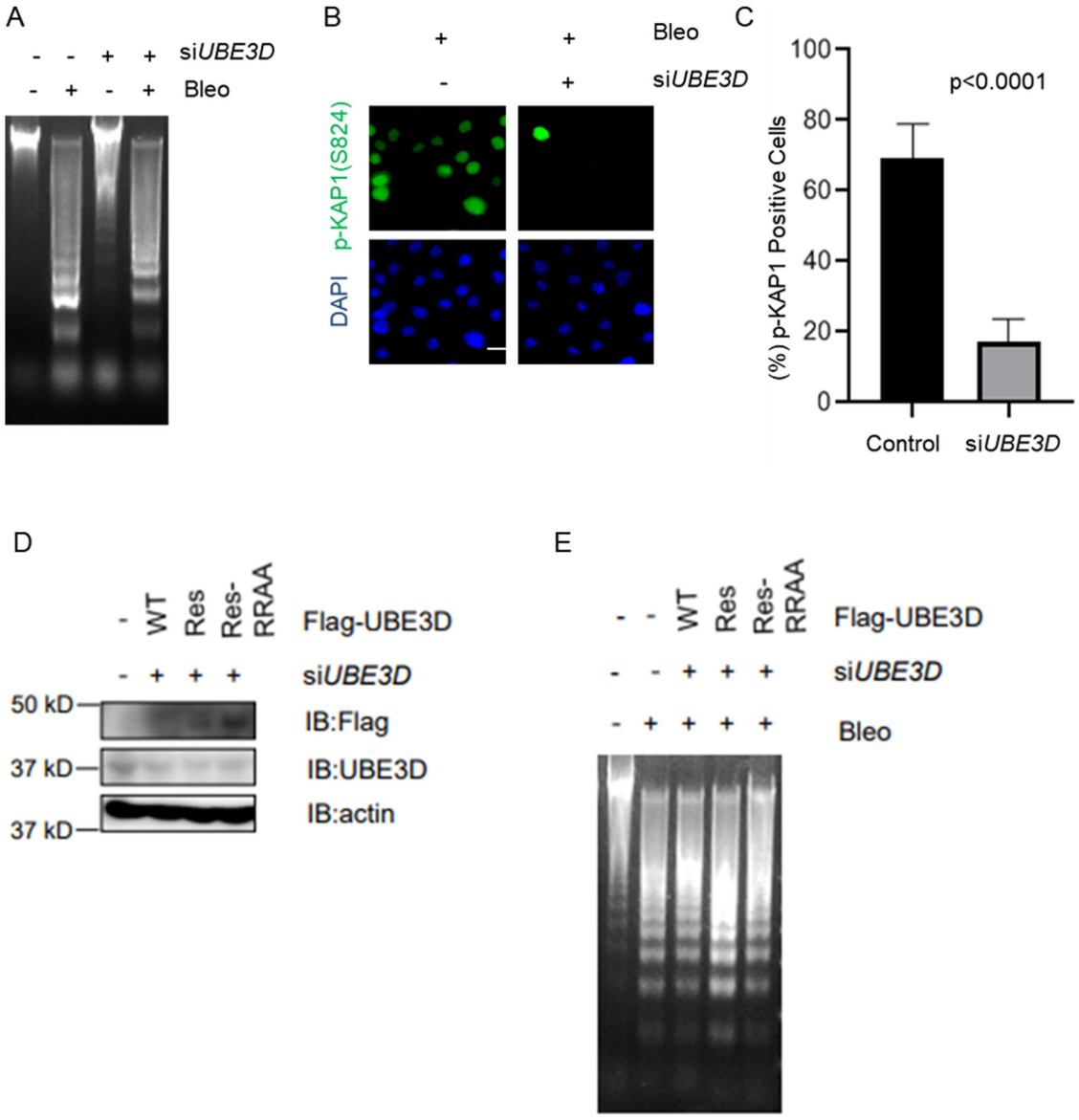

Figure 5. UBE3D modulates heterochromatic homologous recombination. (**A**) UBE3D depletion decreased MNase accessibility of chromatin after Bleomycin treatment. (**B**) Cells were depleted of UBE3D, and then treated with bleomycin. Then, the cells were stained with KAP1-pS824 antibodies and DAPI. Scale bar = 10 µM. (**C**) Quantitation of **B**. At least 100 cells were counted, and the experiments were repeated 3 times. (**D**) Stable transfectants of vec, UBE3D-WT, and –RRAA plasmids in cells after siUBE3D treatment. (**E**) Cells in **B** were subject to the same analysis as in **A**. The histogram represents mean ± SD. $P < 0.001$ (Student's *t*-test).

UBE3D Interacts With KAP1 Through R377R378

We then attempted to pinpoint the interaction domain with KAP1 on UBE3D. A recent investigation illustrated that Ring Finger Protein 4 (RNF4) recruits KAP1 through a conserved Arg-rich motif,[26] therefore we scanned the UBE3D sequence and identified a similar R377R378 moiety.

We constructed UBE3D-RRAA mutants (see Fig. 2H). Cells were transfected with Flag-UBE3D-WT, -RRAA and together with HA-KAP1 plasmids. The subsequent co-immunoprecipitation experiments indicated that the RRAA mutations abolished interaction between KAP1 and UBE3D (Fig. 4A). When pulldown assays were utilized, GST-KAP1 pulled down Flag-UBE3D-WT, but not the –RRAA mutant proteins (Fig. 4B), suggesting that R377R378 are indeed indispensable for associating with KAP1. Hence, V379M weakened interaction with KAP1, but to a lesser degree compared to the RRAA mutant.

As V379M is exactly downstream of R377R378, we surmised that it might also act in the same manner, and hence analyzed it in parallel. In the co-immunoprecipitation experiments, V379M did not display discernable differences as compared to the WT (see Fig. 4A). In the pulldown experiments, the V379M mutation weakened interaction with KAP1 (see Fig. 4B). As methionine could be easily oxidized to methionine sulfoxide (MetSO)[27] and age-related oxidation stress has been ascribed to AMD pathogenesis,[2] we reasoned that oxidation of V379M might be conducive to AMD. To that end, we first treated the recombinant GST-UBE3D-V379M proteins with H_2O_2, and then used the oxidized proteins in the pulldown assays (Fig. 4C). Compared to WT, V379M displayed upshift during gel electrophoresis as

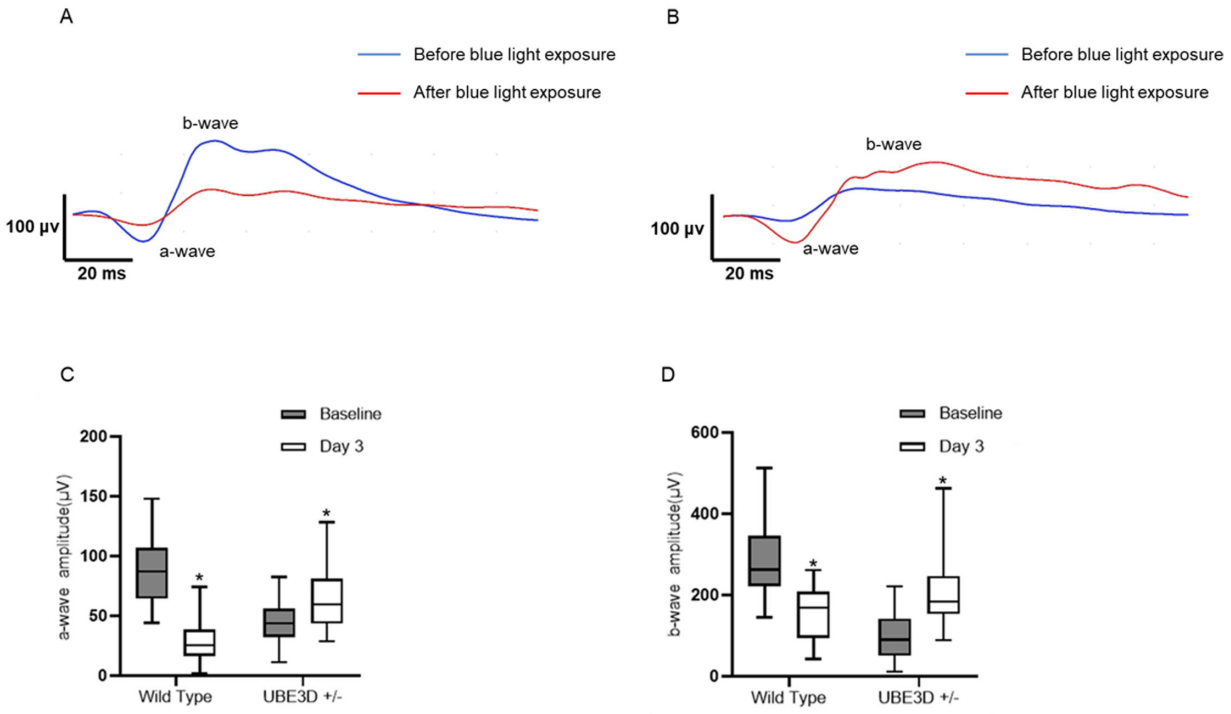

Figure 6. Blue light induces less damage in UBE3D$^{+/-}$ mice than in WT as measured by electroretinography (ERG). The 12-month-old WT and UBE3D$^{+/-}$ mice were induced with blue light damage as described in the Materials and Methods section. The ERG results revealed that the a-wave and b-wave of WT mice decreased (**A**), whereas those of the UBE3D$^{+/-}$ heterozygous mice increased (**B**). Box plots show the pooled data of the WT mice and the UBE3D$^{+/-}$ heterozygous mice in a-wave and b-wave (**C, D**). Data are the means ± SD. * $P < 0.001$ (Student's *t*-test). The number of animals used in these experiments are: WT: $N = 12$; UBE3D$^{+/-}$: $N = 8$.

described before.[28] Intriguingly, V379M reduced interaction with KAP1, with the oxidized protein dampening the association even more (see Fig. 4C). Moreover, we constructed a V379Q mutant, as Q is the structural mimicry of MetSO.[29] Upon ADR induction, UBE3D-WT significantly augmented interaction with KAP1, whereas UBE3D-V379Q substantially debilitated the partnership (Fig. 4D). In sum, UBE3D engages with KAP1 via R377R378. In the V379M mutation, M will be oxidized to become MetSO, thus disrupting the KAP1-UBE3D interaction, probably due to steric hindrance imposed upon the RR motif.

siUBE3D Might Decrease MNase Accessibility of Chromatin After Bleomycin Treatment

Then, we directly measured chromatin de-condensation by micrococcal nuclease (MNase) assays. Bleomycin treatment significantly enhanced MNase accessibility, as previously reported, but the extent of chromatin relaxation is reduced in cells depleted of UBE3D (Fig. 5A). We then examined whether UBE3D is vital for KAP1 recruitment to the DNA damage site. In the WT cells, KAP1-pS824 is readily discernible after bleomycin treatment (Fig. 5B), but the signal is significantly decreased in UBE3D-depleted cells (see Figs. 5B, 5C). We then prepared stable transfectant cells harboring UBE3D-WT and –RRAA mutant plasmids, and the RRAA mutants marked decreased chromatin de-condensation upon DNA damage (Figs. 5D, 5E). These results suggest that UBE3D and more specifically, the interaction between UBE3D and KAP1 are instrumental for DNA damage-induced chromatin relaxation.

Old UBE3D$^{+/-}$ Mice Manifested Less Damage Under Blue Light Exposure

As our biochemical results indicate that oxidation of human UBE3D-V379M might contribute to retinal degeneration, we wondered what would happen in mice. As WT mice harbor M379 and humans harbor V379, we used our generated UBE3D$^{+/-}$ mice to mimic the UBE3D V379M mutation in patients with AMD.[4] We made an educated guess that lack of a copy of V379M might be beneficial for mouse eyes, due to less MetSO production.

Because AMD is characterized by gradual loss of vision, retinal pigment epithelium (RPE) and photoreceptor damage,[30] we took advantage of the blue light-induced eye damage model in mice, as it is a widely used model for studying photoreceptor degeneration.[31] The 12-month-old WT and UBE3D$^{+/-}$ mice were induced with blue light damage, as described in the Materials and Methods section. Then, they were measured for eye damage by ERG and OCT.

ERG is standard to assess eye functional impairment and is the sum of the electrical responses of various nerve cells in the retina. Rod cells and cone cells respond differently to light stimulation with different backgrounds and intensities. Here, we choose flash ERG, namely f-ERG. The a-wave is the initial large negative wave that reflects the function of the outer layer of the retina, mainly photoreceptor cells. The b-wave is the following large positive component that reflects the function of the deep retinal cells. The amplitude of the a-wave represents the function of the photoreceptor, whereas the amplitude of the b-wave reflects the function of the bipolar and Müller cells. Therefore, a decrease in the

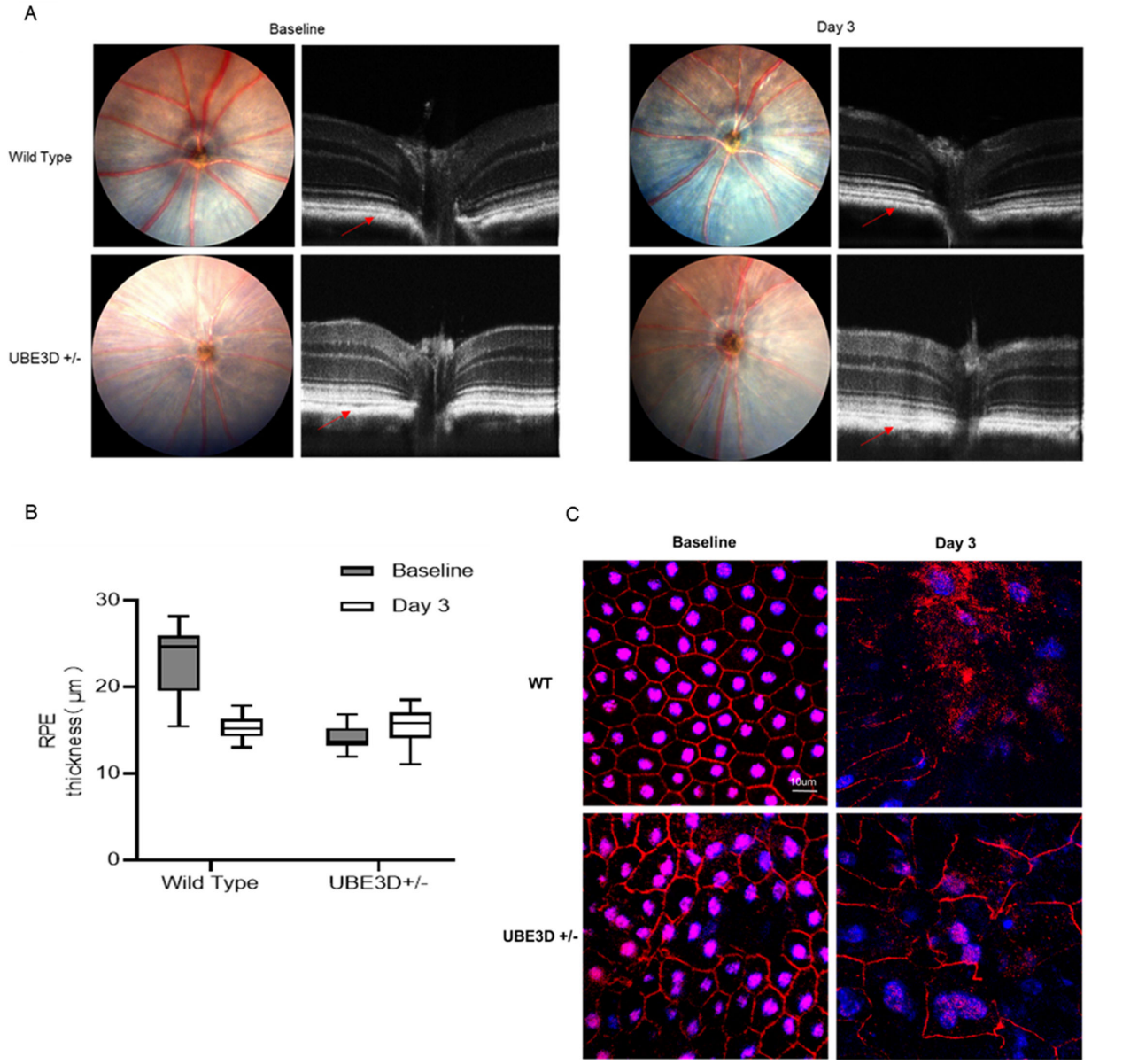

Figure 7. Blue light induces less damage in UBE3D$^{+/-}$ mice than in WT as measured by optical coherence tomography (OCT). (**A**) Fundus photographs and retinal layer thickness determined by OCT. After blue light exposure, the RPE layer (indicated by the *red arrows*) of WT mice became significantly thinner, whereas UBE3D$^{+/-}$ mice became thicker. (**B**) Quantitation of the results in **A**. (**C**) Zonula occludens-1 (ZO-1) images show more severely damaged RPE structures in wild-type mice than in UBE3D$^{+/-}$ mice after the same light exposure. Data are the means ± standard error. *: $P < 0.001$ (Student's *t*-test). The number of animals used in these experiments are: WT: $N = 12$; UBE3D$^{+/-}$: $N = 8$.

amplitude of the a-wave and/or the b-wave indicates retinal dysfunction or improvement, whereas an increase indicates improvement. As revealed in Fig. 6, ERG analysis showed a decrease of the a-wave and b-wave of WT mice, suggesting severe damage to their visual function after exposure to blue light. In UBE3D$^{+/-}$ mice, however, the amplitude of the a-wave and b-wave increased, suggesting that V379M might have a dosage-dependent effect.

Then, we performed fundus photography and OCT on these mice. Fundus photography plays a key role in monitoring the health of eyes. It allows us to see the objective and comprehensive fundus conditions and analyze the changes of the fundus structure. We found that after exposure to the blue light, the RPE layer of WT mice became thinner, whereas that of UBE3D$^{+/-}$ heterozygous mice became thicker. At the same time, we made RPE flat mounts on WT and UBE3D$^{+/-}$ mice before and after blue light exposure, and performed ZO-1 staining and confocal scanning to compare the morphological changes of RPE between the two. We found that the UBE3D$^{+/-}$ mice had some minor RPE damage before light exposure, but after the same light exposure, the RPE damage was lighter than that of the WT group (Figs. 7A-C). These data indicate that the same dose of blue light exposure can cause damage to the physiological structure of the retina in WT mice, which in turn leads to visual impairment; whereas the changes in the structure and function of the retina in UBE3D$^{+/-}$ heterozygous mice will make them more sensitive to light. In sum, in the blue

light eye damage model, old UBE3D$^{+/-}$ heterozygous mice manifested less ocular damage than WT mice.

Discussions

In the human genome, about 95% E3's belong to the really interesting new gene (RING) family, and only 5% or 28 proteins belong to the HECT E3 family.[32] Most of the HECT E3s are not well understood, and UBE3D is one of them. Previously, the only substrate of UBE3D identified in vitro is cyclin B1.[5] Here, we identified a role of UBE3D in the DNA damage repair process. UBE3D is recruited to the damage sites through interacting with PCNA via a PIP box, and binds KAP1 through R377R378, thus mediating the homologous recombination process in the heterochromatin region (Fig. 4E). Intriguingly, both R377R378 and the adjoining V379 are involved in various human diseases, including cancer and AMD.

The pathogenesis of AMD has been varying, ranging from lipid transfer and recycling, phagocytosis defects, extracellular matrix remodeling, and complement activation,[2] but heterochromatic DSB repair is a new comer. Some recent studies have found that DNA damage and repair may be related to AMD.[33,34] Our data suggest that individuals carrying the V379M SNV could be subject to oxidation and the resultant MetSO might dissociate UBE3D from KAP1, thus impairing the DSB repair process. In addition, why it is East Asian-specific is also worthy of further investigation. We speculate that the ethnic brown pupil might absorb more DNA damage-prone sunlight, and entails more repair burdens over the ages compared to other people. We also noted that AMD is an aging-related disease. Because aged cells harbor increased damages and elevated DNA breaks,[35] they might be more prone to DNA damage repair defects.

Our work also suggests a link between oxidative stress and ocular diseases. Our biochemical assays show that oxidation will alter Met to MetSO. Not incidentally, the mouse blue light-induced retinal injury models also involve oxidative stress.[36] Blue light exposure in vitro may also lead to increased expression of oxidative stress-related proteins in cells.[37] As sunlight damage usually comes from ultraviolet (UV) radiation, which might cause reactive oxygen species,[38] a long-term UV exposure might induce oxidative stress. Thus, our animal studies are consistent with biochemical data that oxidative stress plays an important role in AMD pathogenesis.

One question naturally sprung from our work is what is UBE3D doing at the damage sites? Considering UBE3D is an E3 ligase, one could imagine that it could degrade other proteins essential for heterochromatin maintenance, for instance, chromatin remodeling complexes. Indeed, CHD class II nucleosome remodeling complexes, in particular, CHD3.1, has been shown to interact with KAP1 for heterochromatin compaction.[39] It is conceivable that KAP1 would recruit UBE3D to degrade these or other proteins to relax heterochromatin for repair.

Our work also adds a word of caution when exploiting mouse rod cells for DNA damage repair analysis. As previous investigations suggest, adult mouse rods only repair half of the induced DSBs, due to failure to accumulate ATM proteins at the DSBs and decreased KAP1 levels.[22] Currently, mice are widely used as animal models for ocular diseases, perhaps this chromatin context needs to be considered when the disease pathogenesis involves DNA damage repair. In addition, how many eye diseases could be contributed by DNA damage repair? As we are ushering in an exciting new era of genomic medicine, we believe more whole-exome sequencing tests would definitely bring about more disease-susceptible alleles that would tell the whole story.

Acknowledgments

The authors thank Drs. Dongyi Xu (Peking Univ.) and Guohong Li (IBP, CAS) for support and members of the Li laboratory for comments on the manuscript.

Supported by the National Natural Science Foundation of China (NSFC) fund (31872720 to J. L., 81470649 and 81670870 to L.H., 32090031, 31761133012, and 31530016 to X. X.); R&D Program of Beijing Municipal Education Commission (KZ202210028043) to J. L.; Science and technology innovation project of Chinese academy of medical sciences (2019-RC-HL-019) to L.H.; National Key R&D Program of China (2020YFC2008200) to M.Z.; the National Basic Research Program of China (2017YFA0503900), and the Shenzhen Science and Technology Innovation Commission (JCYJ20180507182213033 and JCYJ20170412113009742) to X.X.

Author contributions: Jing L., X.-X. L., L. H, X. X., and G.-H. W. designed the project and analyzed the data. Y. D., L. Jia, and M.-Q. D. performed and analyzed mass spectrometry data. L. H, and N. X. designed and performed the mouse work. Y. L., S. N., Y. T., Q. G., Jie L., and Y. B. performed all other experiments. All authors reviewed and approved the manuscript.

Disclosure: **N. Xu**, None; **Y. Liu**, None; **S. Nai**, None; **Y. Tao**, None; **Y. Ding**, None; **L. Jia**, None; **Q. Geng**, None; **J. Li**, None; **Y. Bai**, None; **G.-H. Wei**, None; **M.-Q. Dong**, None; **L. Luo**, None; **M. Zhao**, None; **X. Xu**, None; **X.-X. Li**, None; **J. Li**, None; **L. Huang**, None

References

1. Martin DF, Maguire MG, Ying GS, Grunwald JE, Fine SL, Jaffe GJ. Ranibizumab and bevacizumab for neovascular age-related macular degeneration. *N Engl J Med*. 2011;364:1897–1908.
2. Fritsche LG, Fariss RN, Stambolian D, Abecasis GR, Curcio CA, Swaroop A. Age-related macular degeneration: genetics and biology coming together. *Annu Rev Genomics Hum Genet*. 2014;15:151–171.
3. Chen M, Luo C, Zhao J, Devarajan G, Xu H. Immune regulation in the aging retina. *Prog Retin Eye Res*. 2018;69:159–172.
4. Huang LZ, Li YJ, Xie XF, et al. Whole-exome sequencing implicates UBE3D in age-related macular degeneration in East Asian populations. *Nat Commun*. 2015;6:6687:1–6.
5. Kobirumaki F, Miyauchi Y, Fukami K, Tanaka H. A novel UbcH10-binding protein facilitates the ubiquitinylation of cyclin B in vitro. *J Biochem*. 2005;137:133–139.
6. Ciccia A, Elledge SJ. The DNA damage response: making it safe to play with knives. *Mol Cell*. 2010;40:179–204.
7. Li J, Xu X. DNA double-strand break repair: a tale of pathway choices. *Acta Biochim Biophys Sin (Shanghai)*. 2016;48:641–646.
8. Downs JA, Nussenzweig MC, Nussenzweig A. Chromatin dynamics and the preservation of genetic information. *Nature*. 2007;447:951–958.
9. Ziv Y, Bielopolski D, Galanty Y, et al. Chromatin relaxation in response to DNA double-strand breaks is modulated by a novel ATM- and KAP-1 dependent pathway. *Nat Cell Biol*. 2006;8:870–876.

10. Goodarzi AA, Noon AT, Deckbar D, et al. ATM signaling facilitates repair of DNA double-strand breaks associated with heterochromatin. *Mol Cell*. 2008;31:167–177.
11. Li J, Wang J, Hou W, et al. Phosphorylation of Ataxin-10 by polo-like kinase 1 is required for cytokinesis. *Cell Cycle*. 2011;10:2946–2958.
12. Peng B, Wang J, Hu Y, et al. Modulation of LSD1 phosphorylation by CK2/WIP1 regulates RNF168-dependent 53BP1 recruitment in response to DNA damage. *Nucleic Acids Res*. 2015;43:5936–5947.
13. Hu QR, Huang LZ, Chen XL, Xia HK, Li TQ, Li XX. X-Linked Retinoschisis in Juveniles: Follow-Up by Optical Coherence Tomography. *Biomed Res Int*. 2017;2017:1704623.
14. Kaneko H, Dridi S, Tarallo V, et al. DICER1 deficit induces Alu RNA toxicity in age-related macular degeneration. *Nature*. 2011;471:325–330.
15. Zhong J, Liao J, Liu X, et al. Protein phosphatase PP6 is required for homology-directed repair of DNA double-strand breaks. *Cell Cycle*. 2011;10:1411–1419.
16. Rouet P, Smih F, Jasin M. Expression of a site-specific endonuclease stimulates homologous recombination in mammalian cells. *Proc Natl Acad Sci USA*. 1994;91:6064–6068.
17. Zhuang Z, Ai Y. Processivity factor of DNA polymerase and its expanding role in normal and translesion DNA synthesis. *Biochim Biophys Acta*. 2010;1804:1081–1093.
18. Seluanov A, Mao Z, Gorbunova V. Analysis of DNA double-strand break (DSB) repair in mammalian cells. *J Vis Exp*. 2010;43:e2002–e2002.
19. Moldovan GL, Pfander B, Jentsch S. PCNA, the maestro of the replication fork. *Cell*. 2007;129:665–679.
20. Sanchez-Molina S, Mortusewicz O, Bieber B, et al. Role for hACF1 in the G2/M damage checkpoint. *Nucleic Acids Res*. 2011;39:8445–8456.
21. Solovei I, Kreysing M, Lanctot C, et al. Nuclear architecture of rod photoreceptor cells adapts to vision in mammalian evolution. *Cell*. 2009;137:356–368.
22. Frohns A, Frohns F, Naumann SC, Layer PG, Lobrich M. Inefficient double-strand break repair in murine rod photoreceptors with inverted heterochromatin organization. *Curr Biol*. 2014;24:1080–1090.
23. Frohns F, Frohns A, Kramer J, et al. Differences in the Response to DNA Double-Strand Breaks between Rod Photoreceptors of Rodents, Pigs, and Humans. *Cells*. 2020;9(4):947–962.
24. Misteli T. Beyond the sequence: cellular organization of genome function. *Cell*. 2007;128:787–800.
25. Noon AT, Shibata A, Rief N, et al. 53BP1-dependent robust localized KAP-1 phosphorylation is essential for heterochromatic DNA double-strand break repair. *Nat Cell Biol*. 2010;12:177–184.
26. Kuo CY, Li X, Kong XQ, et al. An arginine-rich motif of ring finger protein 4 (RNF4) oversees the recruitment and degradation of the phosphorylated and SUMOylated Kruppel-associated box domain-associated protein 1 (KAP1)/TRIM28 protein during genotoxic stress. *J Biol Chem*. 2014;289:20757–20772.
27. Erickson JR, Joiner ML, Guan X, et al. A dynamic pathway for calcium-independent activation of CaMKII by methionine oxidation. *Cell*. 2008;133:462–474.
28. Kato M, Yang YS, Sutter BM, Wang Y, McKnight SL, Tu BP. Redox State Controls Phase Separation of the Yeast Ataxin-2 Protein via Reversible Oxidation of Its Methionine-Rich Low-Complexity Domain. *Cell*. 2019;177:711–721.e718.
29. Drazic A, Miura H, Peschek J, et al. Methionine oxidation activates a transcription factor in response to oxidative stress. *Proc Natl Acad Sci USA*. 2013;110:9493–9498.
30. Fine SL, Berger JW, Maguire MG, Ho AC. Age-related macular degeneration. *N Engl J Med*. 2000;342:483–492.
31. Narimatsu T, Ozawa Y, Miyake S, et al. Disruption of cell-cell junctions and induction of pathological cytokines in the retinal pigment epithelium of light-exposed mice. *Invest Ophthalmol Vis Sci*. 2013;54:4555–4562.
32. Rotin D, Kumar S. Physiological functions of the HECT family of ubiquitin ligases. *Nat Rev Mol Cell Biol*. 2009;10:398–409.
33. Banerjee D, Langberg K, Abbas S, et al. A non-canonical, interferon-independent signaling activity of cGAMP triggers DNA damage response signaling. *Nature Communications*. 2021;12:6207.
34. Zou M, Ke Q, Nie Q, et al. Inhibition of cGAS-STING by JQ1 alleviates oxidative stress-induced retina inflammation and degeneration [published online ahead of print March 28, 2022]. *Cell Death Differ*, https://doi.org/10.1038.s41418-022-00967-4.
35. Misteli T. Higher-order genome organization in human disease. *Cold Spring Harb Perspect Biol*. 2010;2:a000794.
36. Nakamura M, Kuse Y, Tsuruma K, Shimazawa M, Hara H. The Involvement of the Oxidative Stress in Murine Blue LED Light-Induced Retinal Damage Model. *Biol Pharm Bull*. 2017;40:1219–1225.
37. Xia H, Hu Q, Li L, et al. Protective effects of autophagy against blue light-induced retinal degeneration in aged mice. *Sci China Life Sci*. 2019;62:244–256.
38. de Jager TL, Cockrell AE, Du Plessis SS. Ultraviolet Light Induced Generation of Reactive Oxygen Species. *Adv Exp Med Biol*. 2017;996:15–23.
39. Klement K, Luijsterburg MS, Pinder JB, et al. Opposing ISWI- and CHD-class chromatin remodeling activities orchestrate heterochromatic DNA repair. *J Cell Biol*. 2014;207:717–733.

Investigative Ophthalmology & Visual Science